SAND2023-11774R

Plasma Focused Ion Beam Nanothermometry

Sandia National Laboratories is a multimission laboratory managed and operated by National Technology and Engineering Solutions of Sandia, LLC, a wholly owned subsidiary of Honeywell International, Inc., for the U.S. Department of Energys National Nuclear Security Administration under contract DE-NA-0003525.

Sandia National Laboratories
ENERGY
Sandia National Laboratories is a multimission laboratory managed and operated by National Technology & Engineering Solutions of Sandia, LLC, a wholly owned subsidiary of Honeywell International Inc., for the U.S. Department of Energy's National Nuclear Security Administration under contract DE-NA0003525.

LDRD PROJECT NUMBER: 229444
LDRD PROJECT TITLE: Plasma Focused Ion Beam Nanothermometry
PROJECT TEAM MEMBERS: Wyatt Hodges, Julia Deitz, Tim Ruggles, Samantha G. Rosenberg, Joe Boro, Elliot Fowler, Daniel Perry, Mila Nhu Lam, John Williard, Luis Jauregui, Ryan Wixom (PM)

ABSTRACT: In this report we detail demonstration of temperature dependent effects on grayscale intensity imaged in Focused Ion Beam (FIB) microscope, as well as secondary electron (SE) dependence on temperature in the Auger Electron Spectroscopy (AES) and a Scanning Electron Microscope (SEM). In each instrument an intrinsic silicon sample is imaged at multiple temperatures over the course of each experiment. The grayscale intensity is shown to scale with sample temperature. Sample preparation procedures are discussed, along with hypothesized explanations for unsuccessful trials. Anticipated outcomes and future directions for these measurements are also detailed.

INTRODUCTION AND EXECUTIVE SUMMARY OF RESULTS:

As characteristic dimensions of microelectronics shrink, an increased number of components are fabricated on the nanoscale, which leads to decreases in effective thermal conductivity due to truncation of carrier mean free path [1]. This decrease in thermal conductivity from the macroscale diffusion regime increases risk for failure due to hotspots [2]. In order to design around thermal failure, nanoscale measurements of temperature and material properties are becoming increasingly critical. The Basic Research Needs for Microelectronics report from Department of Energy Office of Science Workshop [3] identifies nanoscale thermal management as a need in order to build more energy efficient microelectronics and unleash the potential of Heterogeneously Integrated (HI) systems. The report states that new science for thermal management is needed to handle and manipulate high power densities at device and even atomic length scales. To unlock the potential of nanoscale thermal management, thermometry at the nanoscale (nanothermometry) is needed to map temperatures on the length scales relevant to microelectronics. These same measurements have the potential to probe underlying materials structure via extraction of nanoscale thermal properties. However, this presents a scientific challenge: nanoscale thermometry and nanoscale thermal properties are very difficult to access with existing techniques.

To access the nanoscale regime, electron microscopes hold significant promise. Temperature dependent signals have been shown in transmission electron microscopy (TEM) diffraction patterns of semiconductors [4, 5], however the TEM requires complex sample preparation. Imaging using a scanning electron microscope (SEM) require less onerous sample preparation, and already offer material characterization down to the nanoscale, with

compositional, orientation, and strain mapping [6, 7]. In addition, recent work has demonstrated that secondary electron (SE) emission correlates to temperature in scanning electron microscope (SEM) [8]. This new revelation may mean that it is possible to extract thermal properties and temperature using secondary electron emission, but a better understanding of this relationship will be vital to capitalizing on its potential (i.e. nanoscale thermal/temperature mapping). Furthermore, demonstrating this relationship in the focused ion beam (FIB) opens the possibility of milling through the sample to characterize sub-surface features. Given that most standardized FIBs come equipped with an electron column, the same type of SEM characterization (composition, orientation) is achievable in the same tool. Auger Electron Spectroscopy (AES) tools also frequently utilize an ion beam for milling and an electron column to image sample, another option for this type of characterization.

This report explores utilization of SEM, AES and FIB to observe temperature dependent SE yield, measured by grayscale intensity. These experiments proved challenging to set up correctly, with sample charging and surface contamination impeding observation of the temperature dependent SE emission. Sample charging was the presumed cause of grayscale intensity drift in some unsuccessful trials, but was overcome by grounding the sample to prevent charge buildup. Surface contamination was also a presumed cause of failed trials. To prevent carbon buildup or other surface contamination effects, surface cleaning protocols such as solvent cleaning, surface milling, and plasma cleaning of the vacuum chamber. Successful results were shown for each surface cleaning type. Detector type was also found to have an effect on whether temperature dependence was observed, suggesting an angle dependence for SE emission change as a function of temperature. Due to the short duration of the project, not all combinations of variables were explored.

Despite difficulties in experimental design, temperature dependent effects in the SE yield are observed in all 3 instruments using silicon samples. In the SEM, samples were prepared using solvent cleaning on the surface and temperature dependent grayscale intensity was observed using the through lens detector (TLD). In the AES temperature dependent grayscale intensity was observed with argon milled surfaces and a Channeling Electron multiplier. In the FIB temperature dependent grayscale intensities were observed using both the electron beam and ion beam as excitation sources and plasma cleaned samples. These effects were measured using a TLD for electron beams and both a Everhart-Thornley Detector (ETD) and TLD for the ion beams. Once the surface was milled with gallium ions the electron beam still produced temperature dependent grayscale SE emission as measured by a TLD. These results demonstrate proof of concept of thermometry in electron microscopes in instruments that could be used for 3D characterization utilizing the instruments FIB capabilities.

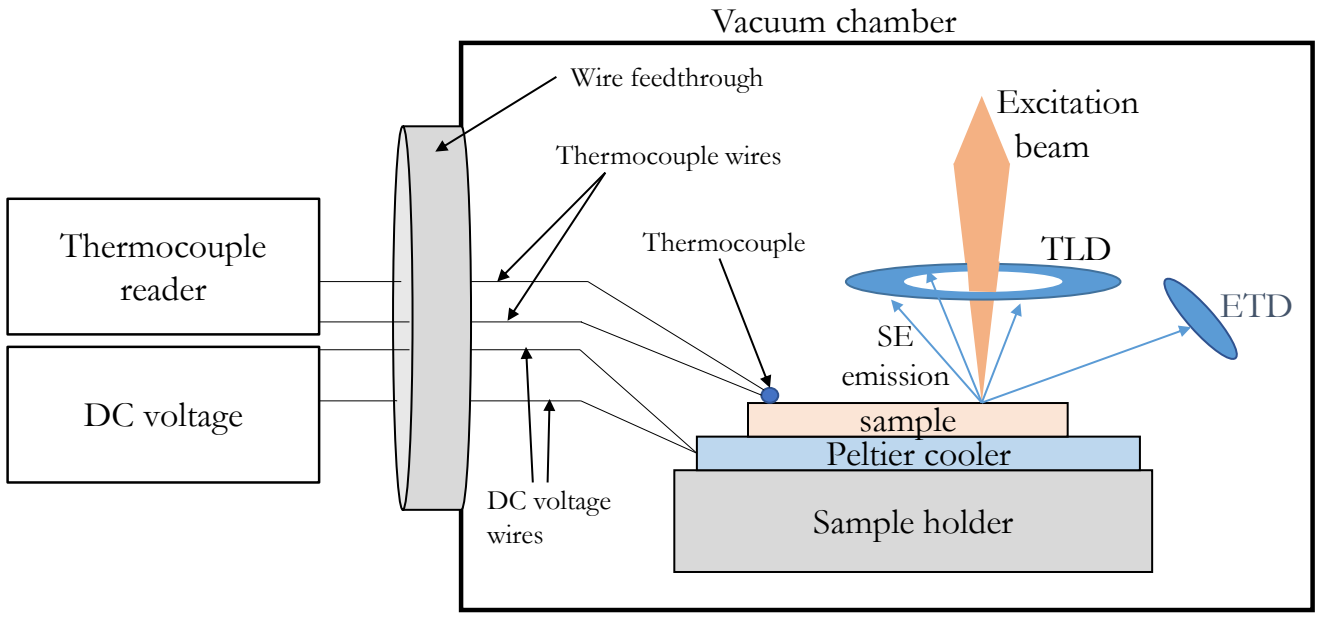

Figure 1: Diagram of experimental setup used in this work. The sample is placed on a Peltier cooler to control temperature. The Peltier cooler is powered with DC voltage, and sample temperature was measured using a thermocouple placed on the sample. The excitation beam hits the sample and the resulting SE emission is measured by a detector, either an ETD or TLD.

DETAILED DESCRIPTION OF RESEARCH AND DEVELOPMENT AND METHODOLOGY:

Temperature dependence of SE emission was tested in 3 instruments: (1) SEM, (2) AES, and (3) a focused ion beam microscope. This section details the general setup used in all 3 instruments, then gives specific details on setup in each microscope individually. The setup described in Figure 1 was used in all microscopes. The sample was mounted to a Peltier cooler for temperature control, with the Peltier cooler mounted to the microscopes sample holder. The Peltier cooler was powered by a DC power supply (Keysight Technologies E3632A) with the wires running through a vacuum feedthrough. A K type thermocouple was then attached to the sample surface in order to monitor the sample temperature. The 2 thermocouple wires were connected to a handheld thermocouple reader (Fluke Model Number 87V/E2), running the thermocouple leads through a vacuum feedthrough. Figure 2 shows a picture of the wire feedthroughs as viewed outside the vacuum chamber of the AES, with the setups in other microscopes working the same way with different electrical feedthrough types.

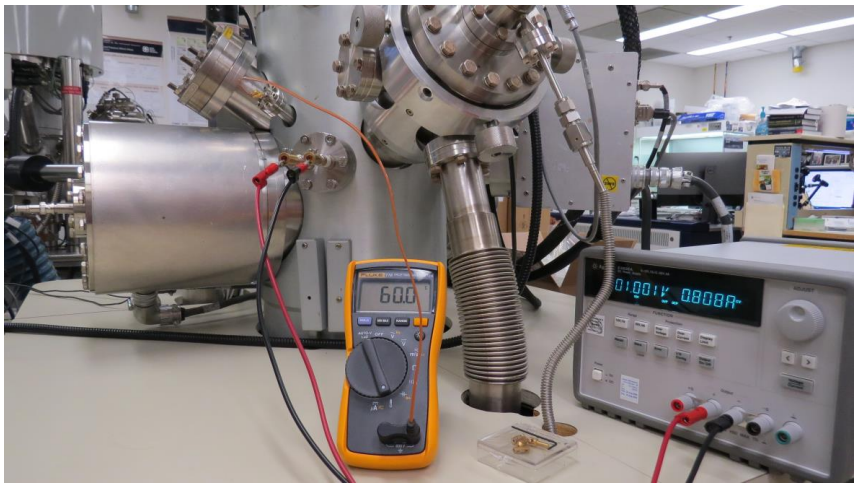

Figure 2: Photograph of the equipment used to apply a DC voltage to the Peltier cooler and measure sample temperature. These are shown with wires running into the vacuum chamber of the AES. Similar equipment was used in the SEM and FIB.

Figure 1 also shows a cartoon picture of the measurement, with the excitation beam (either an electron or ion beam) leading to SE emission from the sample. Two detector types were used for these experiments: the Everhart-Thornley Detector (ETD) which collects backscattered and secondary electrons coming off the sample at an angle, and the Through Lens Detector (TLD) which collects secondary electrons coming back through the excitation beam lens. Both detector types are pictured in Figure 1.

The same procedure was followed to collect data at each point:

1. The voltage supplied by the DC power supply was changed. This caused heating or cooling on the face of the Peltier cooler
2. The experimenters waited until the temperature as measured by the thermocouple reader appeared to stabilize
3. Images were taken for each excitation beam and detector combination of interest
4. The previous steps were repeated until the trial was over

I. Scanning Electron Microscope

SEM trials used a Zeiss Gemini 500 field emission scanning electron microscope. In these tests, the sample was mounted to the Peltier cooler with copper tape, the thermocouple was attached to the sample with Kapton tape. In order to prevent the sample from charging, a piece of copper tape connected the silicon sample to the metal sample holder. A dab of silver paint was used to ensure electrical connection between the sample and the copper tape. The sample was cleaned using acetone, methanol and isopropyl alcohol. The imaging chamber operated at 5e-7 Torr for the duration of the experiment.

Both ETD and TLD detector types were used, but the data using the ETD did not show any temperature dependence. Brightness was set to 50% and contrast was set to 23%. Brightness and contrast values were kept constant for the entire imaging session. Working distance for these images was 10.5 mm, and the XY position of the stage was not adjusted during imaging. A piece of debris was used to focus the image and centered to start the imaging session. The piece of debris moved very little over the course of the imaging. A picture of the sample mounted in the SEM chamber is shown in Figure 3.

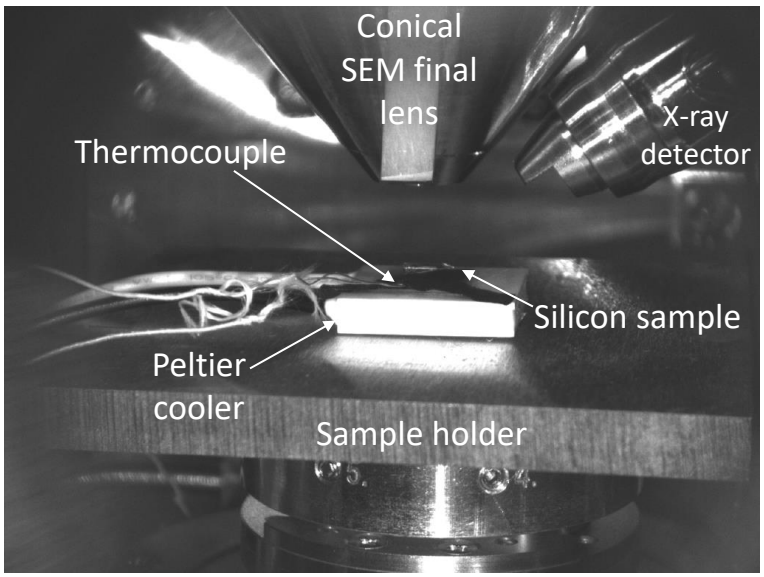

Figure 3: Sample in SEM chamber

II. Auger Electron Spectroscopy

Double sided copper tape was used to mount the silicon sample to the Peltier cooler and to mount the Peltier cooler to the metal sample stage. The thermocouple was affixed to the sample using a metal screw and copper piece. A separate piece of copper provided electrical connection between the sample and metal sample holder. K type thermocouple feedthroughs were used for the thermocouple wires in order to maximize accuracy of the experiment. While pumping down, the Peltier cooler was heated in order to outgas in an attempt to prevent carbon deposition on the sample. The vacuum chamber was pumped down to 5e-9 Torr overnight after mounting the sample and securing the wire leads through the conflat flange feedthroughs. The sample surface was prepared by milling the sample surface 30 nm using an XPS system (Kratos Axis SUPRA). Once the sample was mounted in the chamber and pumped down an Auger spectrum was collected on the sample surface. This spectrum is show in Figure 4, showing very little surface contamination. Imaging was done with a Channeltron Electron Multiplier (CEM). Brightness and contrast settings were kept constant through the entirety of the trial.

(a)

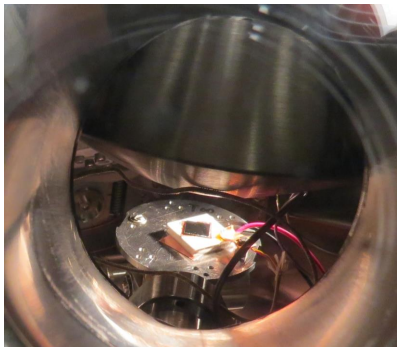

(b)

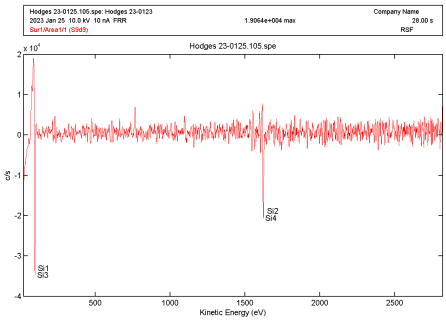

Figure 4: Sample in AES chamber, and collected Auger spectrum of silicon sample.

III. Focused Ion Beam

In FIB trials a FEI D401 dual beam FIB-SEM with a gallium (Ga^+) source was used. The Peltier stage was attached to the sample holder with double sided copper tape. The sample was attached to the Peltier cooler with copper tape in come trials, and silver paint in others. The Thermocouple was attached to the sample using a long strip of Kapton tape. The same wire feedthroughs used for the SEM experiments were used for FIB tests as well. The chamber operated at 5e-7 Torr throughout the experiments. Three measurements were taken at each temperature: (1) excitation with the electron beam and measurement with

7

the TLD, (2) excitation with the gallium beam and measurement with the ETD, and (3) excitation with the ion beam and measurement of SE yield with the TLD. The brightness and contrast were adjusted at the beginning of each trial and kept fixed for the duration of the test. Electron beam accelerating potential was set to 5 keV for all trials, while ion beam accelerating voltage was set to either 5 or 30 keV.

Microscope	Detector	Surface preparation	T-dependent effects observed?
SEM	ETD	Solvent cleaning	No
SEM	TLD	Solvent cleaning	Yes
SEM in AES	CEM	Ar milling	Yes
FIB - electron beam	TLD	Ar milling	Yes
FIB - ion beam	ETD	Ar milling	Yes
FIB - ion beam	TLD	Ar milling	Yes
FIB - electron beam	TLD	Plasma cleaning	Yes
FIB - ion beam	ETD	Plasma cleaning	Yes
FIB - ion beam	TLD	Plasma cleaning	Yes
FIB - electron beam	TLD	Ga milling	Yes
FIB - ion beam	ETD	Ga milling	No
FIB - ion beam	TLD	Ga milling	No

Table 1: Summary of experiments attempted in this project and whether a temperature dependent SE yield was observed.

RESULTS AND DISCUSSION:

Temperature dependent trends were observed in all 3 instruments, with a summary of results in Table 1. The rest of this section details the data collected. All data in figures 5 though 10 are presented in the same way. Subplot (a) plots grayscale intensity with a gray dotted line connecting to the point on the temperature plot. Subplot (b) shows one of the images analyzed in the grayscale intensity plot. Subplot (c) plots grayscale difference between the plotted time and the one before it. Points plotted in red denote when the temperature has increased since the last images, and points plotted in blue denote that temperature has decreased since the last data collection. It is the interpretation of the authors that in the grayscale intensity plots if all red points have the same sign (positive or negative) and all of the blue points have the same sign (positive or negative), then temperature dependent behavior in the grayscale intensity has been observed. The grayscale difference plots have been included to examine the effects of grayscale drift over the course of the experiment, which appears in almost all collected data.

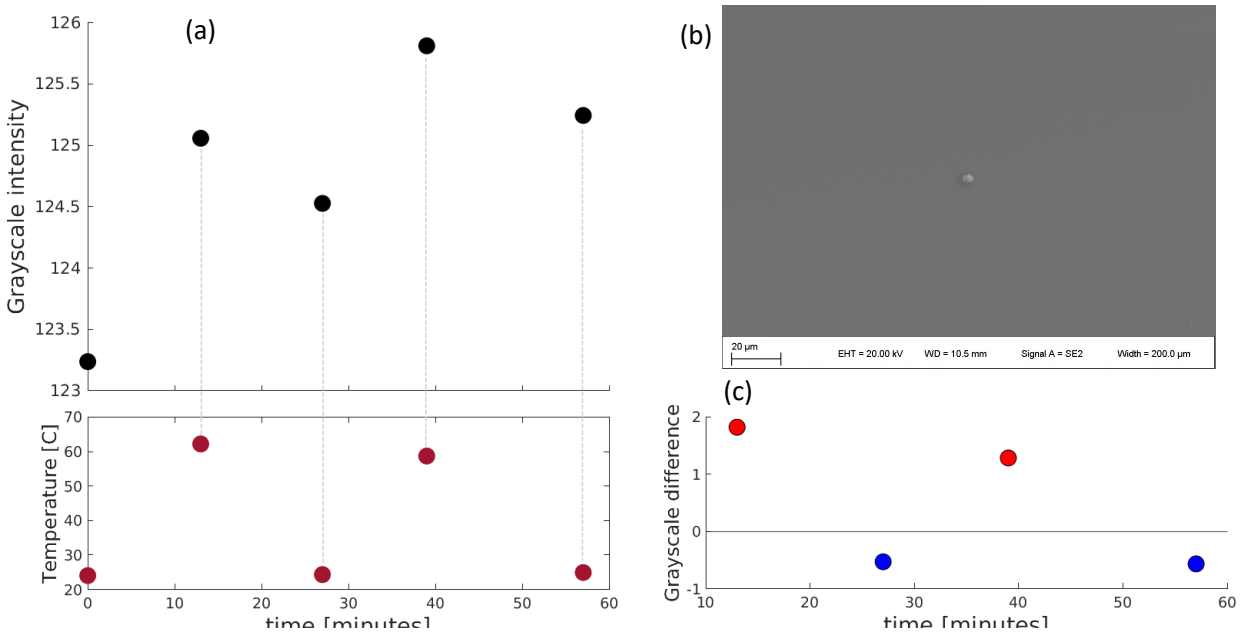

Figure 5: Temperature dependent data in SEM. This trial shows data taken at 30 keV accelerating potential, 120 μm aperture, and 200 μm field of view. (a) shows the grayscale intensity and corresponding temperatures, with gray dotted lines connecting points on the two plots. The sawtooth pattern in Temperature is reflected in the grayscale intensity, through there is drift over the trial. (b) shows one of the images analyzed. (c) Plots grayscale difference between the point plotted and the previous point. Red points represent one in which temperature increased since the last point, and blue point represent one in which sample temperature is lower than the previous point.

I. Scanning Electron Microscope

Several combinations of accelerating voltage, detector type, and aperture were tried in SEM trials. Temperature dependent effects were observed for data using both 5 and 30 keV accelerating potential, as well as both 30 and 120 μm apertures. All data from successful trials looked qualitatively similar to Figure 5, and were collected using the TLD. Unsuccessful trials were attributed to sample contamination, beam drift, and use of the ETD. The sawtooth pattern of the temperature data is reflected in the grayscale intensity, though the grayscale intensity does appear to drift over the course of the trial. It is currently not known what the source of the grayscale drift is. Potential explanations include buildup of contamination on the sample, beam drift, or electrical charging of the sample. The grayscale difference plot shows that when temperature increased, the grayscale intensity also increased, and each time the temperature was decreased, the grayscale intensity also

decreased. This result replicates what has been done in the literature and sets the stage for the other microscopy techniques.

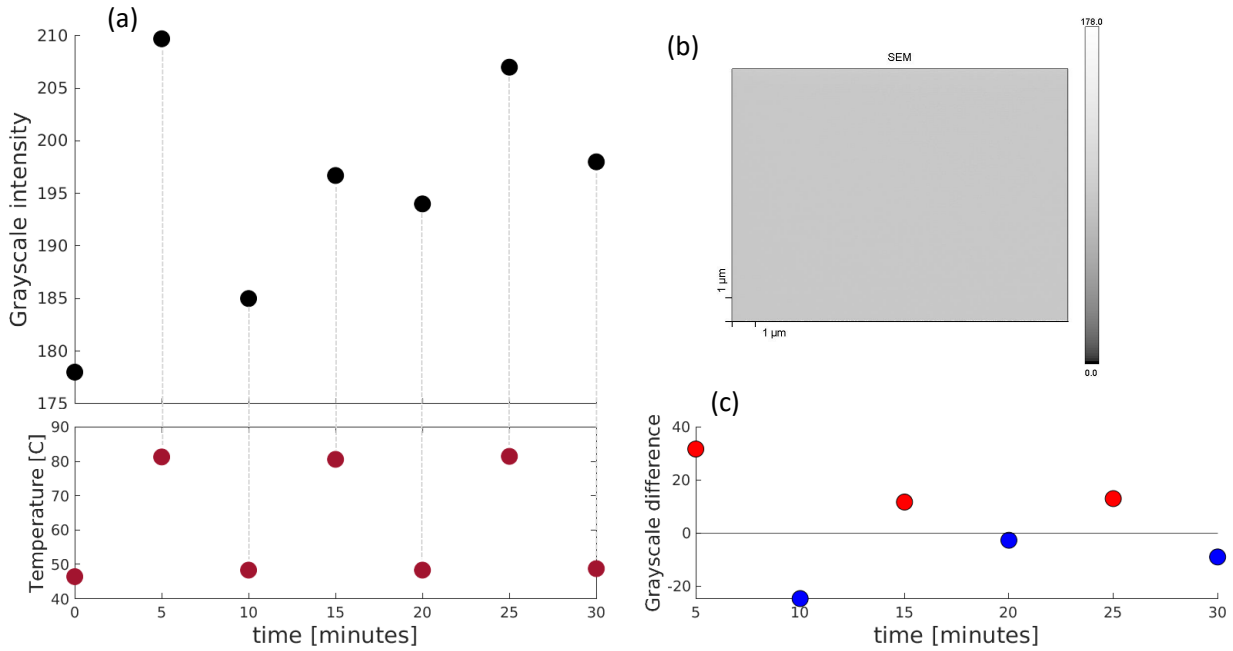

Figure 6: Temperature dependent data in AES. This trial shows data taken at 10 keV accelerating potential, 10 nA beam current, and 20 μm field of view. (a) shows the grayscale intensity and corresponding temperatures, with gray dotted lines connecting points on the two plots. The sawtooth pattern in Temperature is reflected in the grayscale intensity, through there is drift over the trial. (b) shows one of the images analyzed. (c) Plots grayscale difference between the point plotted and the previous point. Red points represent one in which temperature increased since the last point, and blue point represent one in which sample temperature is lower than the previous point.

II. Auger Electron Spectroscopy

Only one test configuration was successfully attempted in the AES. The data for this test is shown in Figure 6. Several other tests encountered issues with ground loops and sample charging. Images of the sample surface were generally very uniform in grayscale intensity, owing to the milling of the sample surface. The sawtooth pattern from the sample temperatures is present in the grayscale data and the grayscale difference does show clear sign differentiation between the points where temperature increased (red points) and the points where temperature decreased from previous measurement (blue points). However, is does

appear that in this trial there is grayscale drift over the course of the experiment. Only one dataset was collected in the project term in part due to the time consuming nature sample preparation and vacuum chamber preparation for these experiments. This system does show promise for future characterization efforts due to the ultra high vacuum capability as well as the ability to mill the sample with inert argon ions.

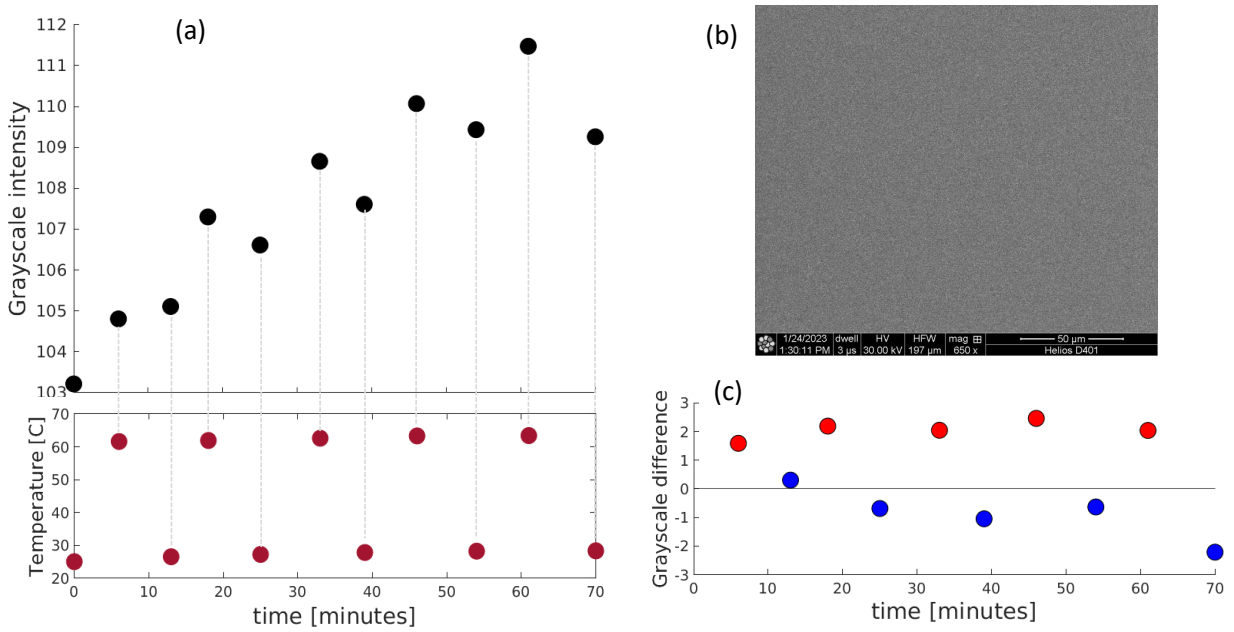

Figure 7: Temperature dependent data in the FIB using the electron beam as the excitation and the TLD to sense SE yield. This trial shows data taken at 30 keV accelerating potential, 2.7 nA beam current, and 200 μm field of view. (a) shows the grayscale intensity and corresponding temperatures, with gray dotted lines connecting points on the two plots. The sawtooth pattern in temperature is reflected in the grayscale intensity, through there is drift over the trial. (b) shows one of the images analyzed. (c) Plots grayscale difference between the point plotted and the previous point. Red points represent one in which temperature increased since the last point, and blue point represent one in which sample temperature is lower than the previous point.

III. Focused Ion Beam

Several test configurations were attempted in the FIB. Unsuccessful tests were attributed to contamination, charging issues, or beam drift. In one case, when temperature of the sample

was taken to 100 C, the Kapton and copper tape lost grip at the high temperature. In the plots shown the sawtooth pattern from temperature increase and decrease was present in data sets from all 3 beam/detector combinations. This trend was present in another trial with low accelerating voltage (5 keV). The data for the electron beam excitation and measurement with the TLD shows an angled sawtooth pattern that trends up with temperature increases, and trends downward when sample temperature decreases. With the exception of the third temperature point, all blue points on the grayscale intensity plot are below zero, and the red points are above zero. The third point shows some of the issue with the amount of drift in these experiments - the increase from the previous temperature is less than the red points. This may indicate that if grayscale drift could be isolated and removed the sawtooth pattern might emerge more clearly.

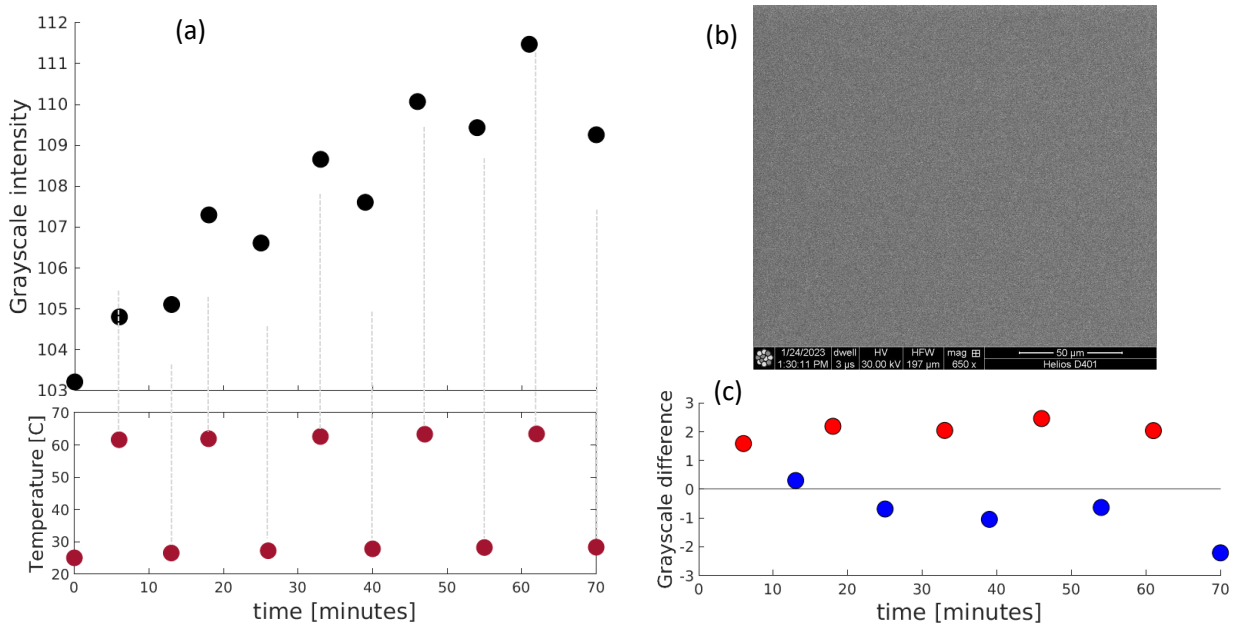

Figure 8: Temperature dependent data in the FIB using the ion beam as the excitation and the ETD to sense SE yield. This trial shows data taken at 30 keV accelerating potential, 0.28 nA beam current, and 200 μm field of view. (a) shows the grayscale intensity and corresponding temperatures, with gray dotted lines connecting points on the two plots. The sawtooth pattern in temperature is reflected in the grayscale intensity, through there is drift over the trial. (b) shows one of the images analyzed. (c) Plots grayscale difference between the point plotted and the previous point. Red points represent one in which temperature increased since the last point, and blue point represent one in which sample temperature is lower than the previous point.

Figure 8 shows the results for excitation with the ion beam and measurement with the ETD. The grayscale intensity does appear to scale with temperature rise, though with the same drift issues that are present in other trials. The first two points do not show the expected trend, one possible explanation for this could be changes in surface chemistry due to interaction with the gallium beam. The grayscale intensity differences between temperature points are around an order of magnitude higher than the grayscale differences in the electron beam trial on the same sample described in Figure 7. This trial demonstrates why ion beam excitation has potential to be more sensitive to temperature changes - the ion beam may lead to increased SE emission in the sample.

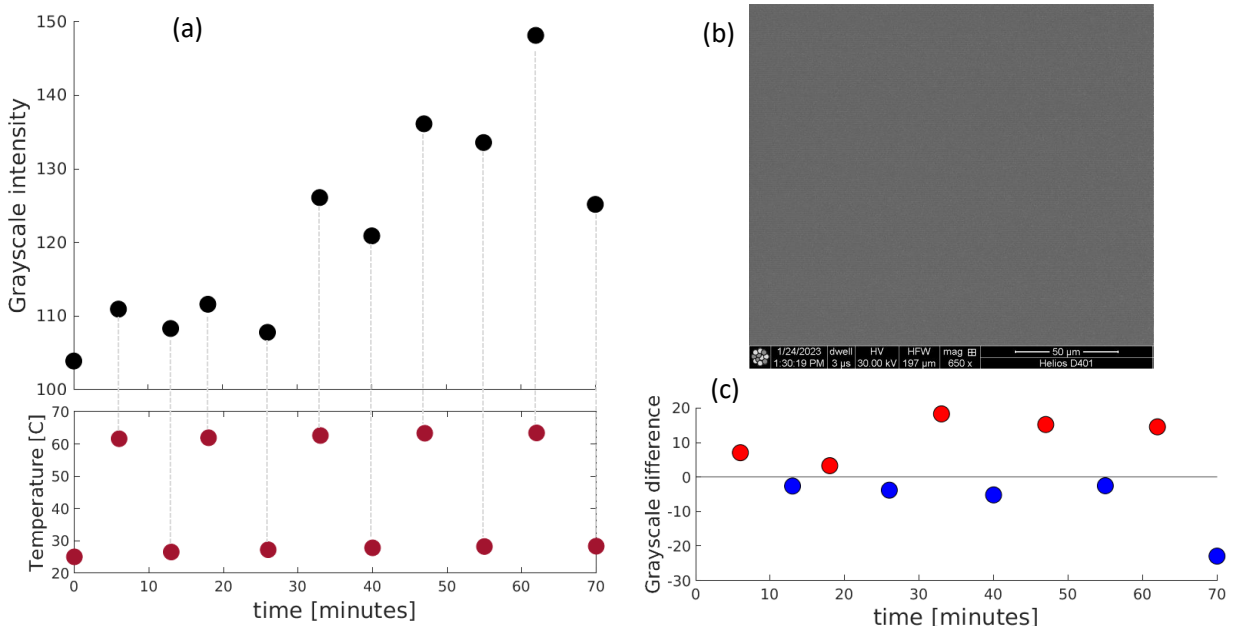

Figure 9: Temperature dependent data in the FIB using the ion beam as the excitation and the TLD to sense SE yield. This trial shows data taken at 30 keV accelerating potential, 0.28 nA beam current, and 200 μm field of view. (a) shows the grayscale intensity and corresponding temperatures, with gray dotted lines connecting points on the two plots. The sawtooth pattern in temperature is reflected in the grayscale intensity, through there is drift over the trial. (b) shows one of the images analyzed. (c) Plots grayscale difference between the point plotted and the previous point. Red points represent one in which temperature increased since the last point, and blue point represent one in which sample temperature is lower than the previous point.

Figure 9 shows results for excitation be the ion beam and SE detection using the TLD. This plot shows the same general trend as the other experiments, with increasing temperature

leading to increased SE as measured by the TLD, and decreasing temperature leading to decreased measured SEs. The magnitude of the grayscale intensity differences are not as high as the ETD trial, suggesting that there is angular dependence on the SE emission. However, the red points on the grayscale difference plot are all above zero and the blue points are all below zero. Since these points were collected third (after Figure 7 and Figure 8), this could be indicative of a more stable surface after the sample was exposed to both the electron beam and ion beam.

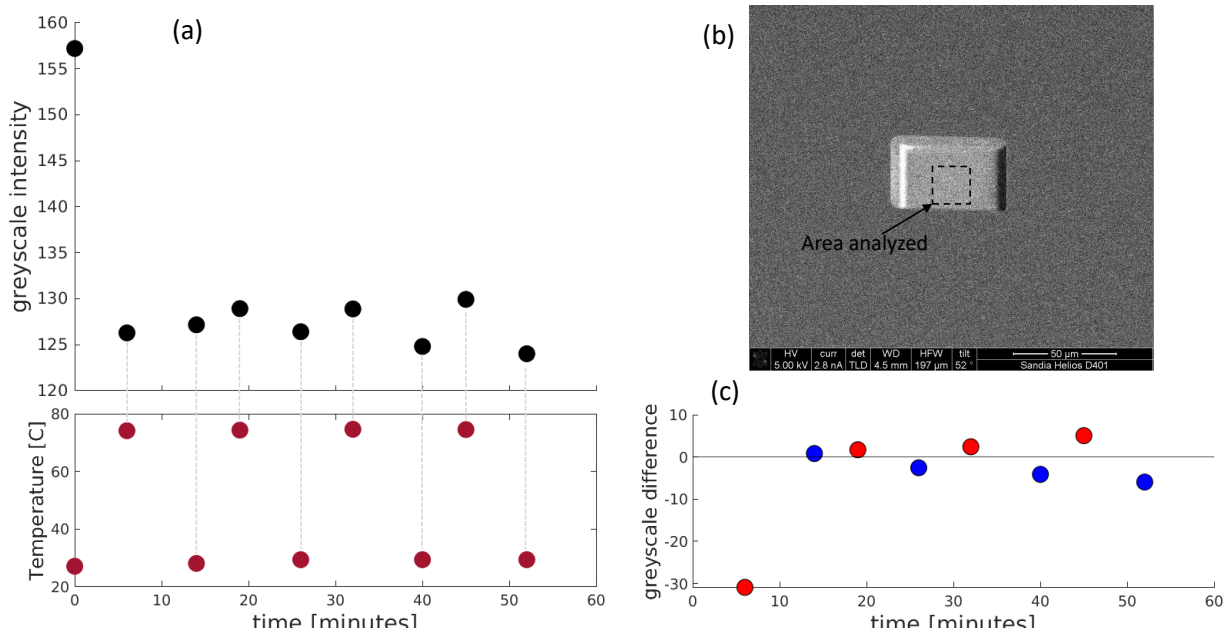

Figure 10: Temperature dependent data in the FIB using the electron beam as the excitation and the TLD to sense SE yield. This trial shows data taken at 30 keV accelerating potential, 2.7 nA beam current, and 200 μm field of view. (a) shows the grayscale intensity and corresponding temperatures, with gray dotted lines connecting points on the two plots. The sawtooth pattern in temperature is reflected in the grayscale intensity, through there is drift over the trial. (b) shows one of the images analyzed. (c) Plots grayscale difference between the point plotted and the previous point. Red points represent one in which temperature increased since the last point, and blue point represent one in which sample temperature is lower than the previous point.

One trial was performed after milling the silicon sample with gallium ions. The milled portion of the sample can be seen in the center of Figure 10 (b). In this trial the ion beam data for both the ETD and TLD did not show temperature dependent behavior. However, the data for which the electron beam excited the sample did not appear to be subject to drift

in the same way as other datasets. This shows promise for preparation by surface milling with gallium ions, as well as shows the robustness of electron beam data in these types of experiments.

ANTICIPATED OUTCOMES AND IMPACTS:

The demonstration of temperature characterization in the SEM, AES, and FIB open up the possibility of many new characterization efforts for microelectronics. Demonstration of temperature dependent SE emission in the AES and FIB is a world first to the best of the authors knowledge. These results will form the basis for submission of a journal paper to Applied Physics Letter and contribute to future conference presentations to heat transfer and microscopy conferences.

This work showed trends in SE yield that were opposite of the literature [8]. This highlights some gaps in understanding the physics of why this change is SE emission occurs in silicon. The opposite trend from literature combined with the ETD not showing temperature dependent yield in the SEM test may suggest that the temperature dependence on SE yield may be angle or even energy dependent. Further isolation of emission angle or SE energy spectrum may give insight on the physics behind temperature dependence of SE emission in different materials. Since all tests in this work were done on intrinsic silicon, different materials may exhibit different SE emission patterns in response to temperature changes. Other materials may also exhibit differences in secondary electron response due to differences in ion interactions with the material, or differences in thermal conductivity of the material due to factors such as doping [9]. These variations may be exploitable for metrology purposes. If SE emission depends on thermal conductivity of the material, defects due to processing may be visible in collected images.

The demonstration of temperature dependent effects in the AES and FIB is significant because of milling capability, showing potential for 3D imaging through repeated cross sectioning and imaging. A partial explanation for drift in the ion beam experiments may be Ga^+ ion implantation. In future work this could be mitigated by using an inert ion such as xenon, which might implant less. Future work may also investigate ways to further mitigate any charging that might be taking place in the experiments. Experiments in which temperature and imaging data are taken during temperature transients could also yield information about the magnitude of temperature dependent grayscale intensity changes as well as information about grayscale drift. More information about drift sources would help determine whether the current qualitative capability could be extended to extract quantitative temperature information.

This work also has the potential to address a gap in the microscopy literature: it is currently not known how hot microelectronics become when hit with the focused ion beam. While estimates have been made [10], their accuracy is unclear. The temperature dependent

nature of SE emission may offer a clue where other techniques cannot. While this path may require calibration for each material that goes in the FIB, in conjunction with modeling it may be able to identify damage during imaging in a way that was not possible before. This future direction may yield new insight to the imaging process.

These results are particularly relevant to DOE Office of Science Programs. Nanoscale thermal management is called out as a research thrust in the 2018 Basic Research Needs for Microelectronics Report [3]. Nanoscale thermal management is identified as key to 3D integration of multiple device layers in heterogeneously integrated systems (PRD 3: Reimagine information flow unconstrained by interconnects), as well as in other research directions (PRD 2:Revolutionize memory and data storage, and PRD 5: Reinvent the electricity grid through new materials, devices, and architectures). Nanothermometry opens up the possibility of identifying hotspots in microelectronics at the scale of current characteristic dimensions of transistors. Qualitative or quantitative temperature data would be useful in hotspot identification. If quantitative temperature data could be extracted from grayscale intensities it could open up characterization possibilities to Sandia such as thermal property extraction at the nanoscale. This type of work could be done in conjunction with microelectronics design and fabrication teams in order to help facilitate faster understanding of the shortcomings of fabricated devices and fabrication processes. Thermal conductivity at the nanoscale may be characterizable in a device using electron microscopes to map temperature at the nanoscale combined with an external heat source or using an active device. These types of characterization techniques would help the NNSA through better process design for microelectronics fabrication as mission relevant devices become smaller and smaller.

Follow on funding to investigate the potential of AES and FIB imaging will be pursued from the DOE SC from future calls on microelectronics design, fabrication, and characterization, as well as the Sandia LDRD office.

CONCLUSION:

SE emission from silicon was measured in SEM, AES, and FIB instruments. Temperature dependence for measured SE yield was observed in all three instruments, with these effects in AES and FIB being world first observations. Surface preparation of the sample, sample grounding, and detector type were observed to have strong effects on the observation of temperature dependent behavior. This work demonstrated proof of concept that the AES and FIB can both measure temperature of semiconductor samples as well as mill the surface. Characterization of this type has the potential to produce temperature maps and identify hotspots on the length scale of current transistors in microelectronic devices. Future work is needed to optimize sample preparation for imaging as well as understand the physics behind the temperature dependence of SE emission in semiconductors.

References

[1] Fan Yang and Chris Dames. Mean free path spectra as a tool to understand thermal conductivity in bulk and nanostructures. *Physical Review B*, 87(3):035437, 2013.

[2] Eric Pop and Kenneth E. Goodson. Thermal Phenomena in Nanoscale Transistors. *Journal of Electronic Packaging*, 128(2):102–108, 12 2006.

[3] Cherry Murray, Supratik Guha, Dan Reed, Gil Herrera, Kerstin Kleese van Dam, Sayeef Salahuddin, James Ang, Thomas Conte, Debdeep Jena, Robert Kaplar, et al. Basic research needs for microelectronics: Report of the office of science workshop on basic research needs for microelectronics. Technical report, USDOE Office of Science (SC)(United States), 2018.

[4] Geoff Wehmeyer, Karen C Bustillo, Andrew M Minor, and Chris Dames. Measuring temperature-dependent thermal diffuse scattering using scanning transmission electron microscopy. *Applied Physics Letters*, 113(25):253101, 2018.

[5] Li He and Robert Hull. Quantification of electron–phonon scattering for determination of temperature variations at high spatial resolution in the transmission electron microscope. *Nanotechnology*, 23(20):205705, 2012.

[6] Joseph I Goldstein, Dale E Newbury, Joseph R Michael, Nicholas WM Ritchie, John Henry J Scott, and David C Joy. *Scanning electron microscopy and X-ray microanalysis*. Springer, 2017.

[7] T. Ruggles, S. Grutzik, K Stephens, and J. Michael. Determining stress in metallic donducting layers of microelectronic devices using high resolution electron backscatter diffraction and finite element analysis. *Microscopy and Microanalysis*, accepted, 2023.

[8] M. I. Khan, S. D. Lubner, D. F. Ogletree, and C. Dames. Temperature dependence of secondary electron emission: A new route to nanoscale temperature measurement using scanning electron microscopy. *Journal of Applied Physics*, 124(19):195104, 2018.

[9] Yongjin Lee and Gyeong S. Hwang. Mechanism of thermal conductivity suppression in doped silicon studied with nonequilibrium molecular dynamics. *Phys. Rev. B*, 86:075202, Aug 2012.

[10] Joseph R. Michael, Daniel L. Perry, Damion P. Cummings, Jeremy A. Walraven, and Matthew B. Jordan. Focused ion beam preparation of low melting point metals: Lessons learned from indium. *Microscopy and Microanalysis*, 28(3):603610, 2022.